Journal of Biomechanics 74 (2018) 72–78

Contents lists available at ScienceDirect

Journal of Biomechanics

journal homepage: www.elsevier.com/locate/jbiomech
www.JBiomech.com

Microscale frictional strains determine chondrocyte fate in loaded cartilage

Edward D. Bonnevie [a], Michelle L. Delco [b], Lena R. Bartell [c], Naveen Jasty [a], Itai Cohen [c], Lisa A. Fortier [b], Lawrence J. Bonassar [a,d,*]

[a] Sibley School of Mechanical and Aerospace Engineer, Cornell University, Ithaca, NY, USA
[b] Department of Clinical Sciences, College of Veterinary Medicine, Cornell University, Ithaca, NY, USA
[c] Applied Engineering Physics, Cornell University, Ithaca, NY, USA
[d] Meinig School of Biomedical Engineering, Cornell University, Ithaca, NY, USA

ARTICLE INFO

Article history:
Accepted 14 April 2018

Keywords:
Mitochondria
Apoptosis
Lubrication
Strain mapping

ABSTRACT

Mounting evidence suggests that altered lubricant levels within synovial fluid have acute biological consequences on chondrocyte homeostasis. While these responses have been connected to increased friction, the mechanisms behind this response remain unknown. Here, we combine a frictional bioreactor with confocal elastography and image-based cellular assays to establish the link between cartilage friction, microscale shear strain, and acute, adverse cellular responses. Our incorporation of cell-scale strain measurements reveals that elevated friction generates high shear strains localized near the tissue surface, and that these elevated strains are closely associated with mitochondrial dysfunction, apoptosis, and cell death. Collectively, our data establish two pathways by which chondrocytes negatively respond to friction: an immediate necrotic response and a longer term pathway involving mitochondrial dysfunction and apoptosis. Specifically, in the surface region, where shear strains can exceed 0.07, cells are predisposed to acute death; however, below this surface region, cells exhibit a pathway consistent with apoptosis in a manner predicted by local shear strains. These data reveal a mechanism through which cellular damage in cartilage arises from compromised lubrication and show that in addition to boundary lubricants, there are opportunities upstream of apoptosis to preserve chondrocyte health in arthritis therapy.

1. Introduction

Under healthy conditions, articular cartilage provides joints with the most efficient bearing surface found in nature. However, the failure of this tissue in osteoarthritis (OA) is the leading cause of severe disability in the United States (Murphy et al., 2008). Despite its widespread prevalence, early stages of OA and its progression are not well understood (Anderson et al., 2011; Buckwalter et al., 2013). Even in cases with a known initiating event such as a traumatic injury, symptomatic OA can take decades to manifest (Brown et al., 2006) obscuring mechanisms leading to the initiation of dysfunction. This knowledge gap arises from an incomplete understanding of how mechanical perturbations dictate biological responses in the early stages of disease (Buckwalter et al., 2013).

There is mounting experimental evidence that friction acutely affects chondrocyte homeostasis (Waller et al., 2013). Cartilage exposed to high friction exhibits significantly more chondrocyte apoptosis compared to cartilage lubricated by healthy synovial fluid (Waller et al., 2013). Such findings indicate that elevated cartilage friction coefficients increase shear strains (Wong et al., 2008), a known correlate to cell death. From these previous findings, a picture emerges where factors such as aging (Temple-Wong et al., 2016), traumatic injury (Elsaid et al., 2008), and disease (Kosinska et al., 2015) affect levels of lubricants such as lubricin and hyaluronic acid in synovial fluid, which in turn increases the friction coefficient at the cartilage surface (Bonnevie et al., 2015; Schmidt et al., 2007). However, the relationship between elevated friction, frictional shear strains, and adverse cellular responses such as apoptosis is not clear.

Mechanically-mediated apoptosis often progresses through mitochondria-driven processes (Wang and Youle, 2009). In these cascades, excessive intracellular calcium leads to mitochondrial depolarization, and mitochondrial depolarization can initiate caspase activation though cytochrome C release (Huser and Davies, 2007). Recent evidence suggests that excessive friction can play a role in initiating this cascade, as lubricin knock-out (i.e., lubrication

* Corresponding author at: 149 Weill Hall, 526 Campus Rd., Ithaca, NY 14853, USA.
E-mail address: Lb244@cornell.edu (L.J. Bonassar).

https://doi.org/10.1016/j.jbiomech.2018.04.020
0021-9290/

inhibition) leads to mitochondrial dysregulation (Waller et al., 2017). However, it is unclear whether this cellular dysregulation is dependent on friction-mediated mechanics. In part, this knowledge gap arises due to the difficulty of measuring friction coefficients, the resulting microscale mechanics and cellular response in a single tissue source. To address this missing link regarding the role of friction and the resulting mechanics that stimulate chondrocyte dysfunction, we combined a frictional bioreactor with confocal elastography and image-based cellular assays to establish the link between cartilage friction, micro-scale shear strain, and acute, adverse cellular responses.

2. Methods

2.1. Tissue harvest and preparation

Cartilage from the femoral condyles of more than 10 neonatal bovids were collected within 24 h of sacrifice (Gold Medal Packing, Rome NY). Cylindrical plugs (6 mm diameter by 2 mm thick) were extracted using sterile practices from the central region of the condyles along the major axis of articulation. Prior to any mechanical stimulus, samples were equilibrated for 90 min in Dulbecco's Modified Eagle Medium (DMEM) at 37 °C and 5% CO_2. Synovial fluid was extracted from healthy adult horses and pooled from several joints to minimize sample to sample variability.

2.2. Frictional sliding

Articular cartilage samples were slid against polished glass counterfaces (McMaster Carr, Elmhurst, IL) in a custom-built tribometer (Bonnevie et al., 2015; Gleghorn and Bonassar, 2008) (SFig. 1A). Samples were submerged in a lubricating bath of either phosphate buffered saline (Corning, Manassas VA) or equine synovial fluid. Samples were compressed to 15% axial strain using optical micrometer stages (10 μm resolution) before sliding 30 reciprocating cycles of ±6 cm at 1 mm/s as actuated by a lead screw-driven stage actuated by a micro-stepper motor (MDrive Plus, Schneider Electric, Rueil-Malmaison, France). Both shear and normal loads were collected simultaneously using a custom biaxial load cell and friction coefficient was calculated as the ratio between shear load and normal load and averaged across the sliding cycle.

2.3. Depth-dependent shear strain measurements

A setup emulating the tribometer configuration (Fig. 1A) was mounted on a Zeiss Live 5 confocal microscope to measure depth-dependent frictional shear strains. Shear strains were tracked in a similar manner to previous studies that measured depth-dependent shear properties (Buckley et al., 2010; Griffin et al., 2014). Samples were axially bisected to form hemicylindrical samples that were mounted via their deep zone using cyanoacrylate adhesive to a tissue deformation imaging stage as previously described (Buckley et al., 2010). Samples were stained for 30 min in 7 μg/mL 5-DTAF for general protein florescence followed by PBS washes. In contrast to our previous studies, samples were bathed in either PBS or synovial fluid and compressed to 15% axial strain against polished glass using a micrometer stage. In a similar manner to frictional testing, the glass slide was reciprocated against the cartilage surface using a piezoelectric positioning stage actuated with an average speed of 1 mm/s. Videos were captured at 20 frames per second focused near the tissue surface to track the depth dependent shear strains (See supplemental videos). Depth-dependent shear deformations were tracked by analyzing the displacements photo-bleached lines perpendicular to the articular surface. The maximum local shear strains were calculated through differentiation of the local displacements as previously described (Buckley et al., 2010).

2.4. Cellular imaging

Viable, hydrated cartilage explants were imaged on a Zeiss LSM 710 confocal microscope to determine the cellular responses to repeated frictional shear. After 30 cycles of sliding, samples were either incubated in DMEM for 2 h before staining, or incubated for 24 h in DMEM supplemented with 100 U/ml penicillin and 100 μg/ml streptomycin. Live/Dead staining was conducted 2 h after sliding. Cylindrical samples were axially bisected into hemicylinders and stained for 20 min with 4 μM Calcein AM and 2 μM Ethidium homodimer (Molecular Probes) followed by PBS rinse. Calcein AM and Ethidium homodimer were both excited by a 488 nm laser line (7% power) and differentiated upon spectrally resolved detection into channels set for green (493–574 nm) and red (590–740 nm) which were available as presets in the Zen software (Zeiss) for the respective fluorophores. Control and frictionally loaded samples were scanned at the same time points with the same imaging parameters. Mitochondrial polarization was assessed 2 h after sliding as well. Hemicylindrical samples were stained with MitoTracker Green (MTrG; 200 nM) for 40 min followed by 20 min with tetramethylrhodamine methyl ester perchlorate (TMRM; 10 nM) added. Briefly, MTrG staining was used to stain all MT, regardless of membrane polarity, whereas TMRM staining was used to indicate functional (i.e., polarized) MT. Additionally, samples incubated for 24 h after sliding were stained with CellEvent Caspase-3/7 Green (Thermo Fischer Scientific) following manufacturer instructions. Staining for 30 min was conducted before imaging along with confocal reflectance.

Depth-dependent cellular responses were quantified using ImageJ. Confocal images were imported into ImageJ, and segmented into 7 depth dependent bins (50 μm depth by 250 μm wide) with all cells analyzed per bin (~50 cells/bin; ~350 cells were analyzed per sample). Image analysis outcomes were reported as percentage cell death (*100 ∗ total red cells/total red and green cells*), percent cells with depolarized MT (*100 ∗ total green cells/total cells colocolizing red and green)*, and number of caspase-positive cells.

2.5. Statistical analyses

Differences in equilibrium friction coefficient were determined by Student's *t*-test for the 30th cycle of sliding. Differences in depth-dependent shear strain were determined at each depth similarly with a Student's *t*-test and average p value was reported for all depths in addition to the max p value (i.e., least significant). Cellular effects between lubrication groups and control were analyzed using non-linear mixed effects models. Treatment group (Control, PBS, or Synovial Fluid) and depth (50, 100, 150, 200, 300, and 350 μm) were analyzed as fixed effects, and animal was considered a random effect. Cellular responses as a function of depth were fit to exponential models (i.e., Response = $A * e^{-depth/B}$, where *A* and *B* are fitting parameters with fixed and random effects). The residuals were assessed for normality and homogeneity. P-values were used to assess differences in amplitude (A) and decay rate (B) between groups. Correlations between measured parameters were determined using a Pearson correlation coefficient. Further details of this analysis are available in the supplemental material and Supplemental Table 1. Significance was set at $p < 0.05$, and all analyses were conducted in Excel or Matlab.

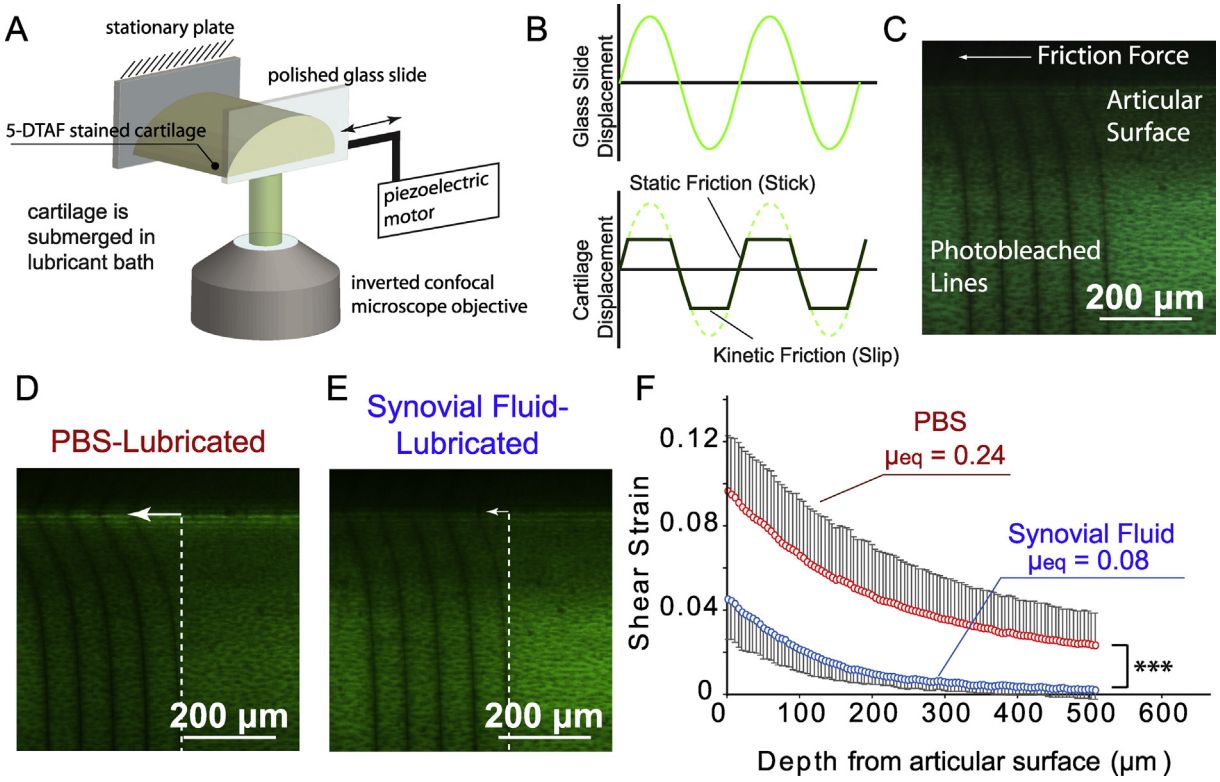

Fig. 1. Friction causes depth dependent shear strains within the cartilage matrix. (A and B) Cartilage was mounted on an inverted confocal microscope, compressed to 15% axial strain, and a glass slide was slid against the surface while depth-dependent deformations were tracked. (C) Photobleached lines provided fiducial markers to track depth-dependent deformations. (D and E) Representative snap shots of maximum cartilage deformation under friction. Arrows denote degree of surface deflection. (F) Shear strain for PBS was at least twice as high as synovial fluid throughout the cartilage depth ($^{***}p < 0.005$, n = 7–8). Error bars represent mean + or − standard deviation.

3. Results

3.1. Amplified shear strains in the cartilage superficial zone

To establish how friction applied to the articular surface induces microscale strains we compared friction coefficient measurements from a frictional bioreactor with local shear strain measurements obtained from confocal elastography. Samples compressed to physiologic strain levels (Carter et al., 2015) and slid for 30 cycles over 1 h at 1 mm/s while bathed in either phosphate buffered saline (PBS) or in synovial fluid exhibited significantly different friction coefficients. Additionally, the friction coefficient for both lubricants exhibited time dependence as expected (Ateshian, 2009) and reached equilibrium values after ~15 cycles (Supplemental Fig. 1). At equilibrium, the coefficient of friction for PBS was 2.8 times that of synovial fluid ($p < 0.008$, $\mu_{eq} = 0.25 \pm 0.02$ for PBS lubricated cartilage and $\mu_{eq} = 0.09 \pm 0.05$ for synovial fluid lubricated cartilage, n = 3 per group). This cartilage-on-glass configuration was mounted on a confocal microscope (Fig. 1A) and videos were collected of cartilage articulated in either PBS or synovial fluid (Fig. 1B–E). The increase in friction for cartilage lubricated by PBS, in turn, generated significantly higher shear strains. Throughout the depth, shear strain in PBS-lubricated cartilage was at least twice as high as those of synovial fluid-lubricated cartilage ($p_{ave} < 0.001$, $p_{max} = 0.0026$, n = 7–8 samples per group, p values calculated at 96 depths, Fig. 1F). Due to the depth-dependent, graded structure of cartilage, both PBS- and synovial fluid-lubricated cartilage exhibited depth-dependent shear strain with large strains primarily concentrated in the superficial zone, within 100 μm of the articular surface (Buckley et al., 2010; Wong et al., 2008). For PBS-lubricated cartilage, shear strain reached a maximum of 9.7 ± 2.6%, while the maximum strain in the synovial fluid-lubricated cartilage peaked at 4.5 ± 1.9%. These data show that the effects of increased friction are particularly concentrated near the articular surface. Recent studies have shown that cell death is highly correlated to excessive local strains (Bartell et al., 2015). As such, it is important to determine whether such depth dependent differences in induced strains between lubricant groups affect chondrocyte homeostasis.

3.2. Depth-dependent chondrocyte homeostasis

To determine how chondrocyte homeostasis varies with depth from the tissue surface, we assayed samples that underwent 30 cycles of sliding over 1 h in the frictional bioreactor 2 h post sliding (Fig. 2A–D). Samples were analyzed for both lubricant- and depth-dependence for acute cell death (n = 4 biological replicates per group, analyzed in 7 × 50 μm deep bands with ~50 cells per bin, ~350 cells per sample). Staining with both Calcein AM (live, green) and ethidium homodimer (dead, red) revealed minimal cell death in control tissue. In tissue lubricated by synovial fluid, <10% of cells died except in the superficial most 50 μm of the tissue, where 26 ± 9% of cells died. In contrast, cartilage lubricated by PBS exhibited significantly more cell death than control and synovial fluid-lubricated cartilage. Specifically, within the first 50 μm of tissue, almost all (95 ± 4%) cells were dead, and between 50 and 100 μm deep, close to half (40 ± 15%) of the cells were dead. This effect of acute cell death rapidly decays deeper into the tissue, with fewer than 10% of cells located deeper than 150 μm from the articular surface experiencing acute cell death. These results suggest that in cartilage exposed to high friction, the relatively large strain induced in the superficial zone surpassed the threshold to induce acute chondrocyte death.

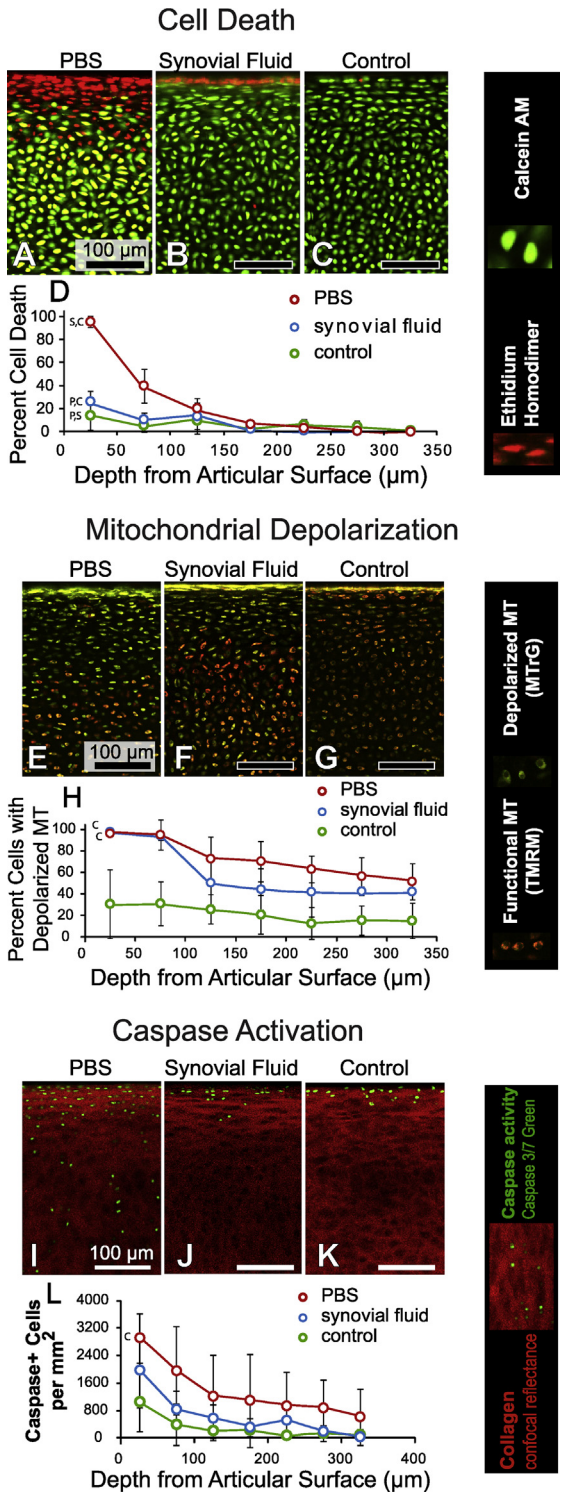

Fig. 2. Depth-dependent cellular responses are associated with elevated friction. (A–C) Live/Dead staining of PBS, synovial fluid, and control cartilage revealed significant cell death in PBS-slid cartilage. (D) Percent cell death was significantly higher for PBS than the other two groups ($p < 0.001$), and for synovial fluid compared to control ($p < 0.01$, $n = 4$ per group). (E–G) Significant mitochondrial depolarization was revealed in the superficial most 100 μm of both PBS- and synovial fluid-lubricated cartilage. (H) Lubricant and depth-dependence of MT depolarization. Significantly more MT depolarization was detected in cartilage slid in PBS and synovial fluid compared to controls ($p < 0.001$, $n = 4$ per group). (I–K) Active caspase 3/7 imaged 24 h after sliding. (L) PBS-lubricated cartilage exhibited significantly more apoptotic cells compared to control ($p < 0.01$, $n = 4$ per group). Error bars depict mean ± standard deviation. Letters denote significant differences in amplitude of responses between group and C – control, S – synovial fluid, and P – PBS. For more information on statistical analyses, see supplemental Fig. 3.

To address whether cells exposed to sub-necrotic levels of strain trigger alternative cellular responses, we assayed mitochondrial dysfunction, a factor emerging as an early indicator of cartilage degeneration (Delco et al., 2017; Goetz et al., 2016; Waller et al., 2017). We measured mitochondrial polarization 2 h post sliding by staining all mitochondria with MitoTracker Green and functional mitochondrial membranes with the membrane-polarity-sensitive dye tetramethylrhodamine methyl ester perchlorate (TMRM; 10 nM). Similarly to the acute cell death response, a significant portion of cells exhibited mitochondrial dysfunction, or more specifically depolarization of mitochondrial membranes as evidenced by a lack of TMRM staining. This MT depolarization was both depth- and friction-dependent (Fig. 2E–H). Within the superficial-most 100 μm, both PBS- and synovial fluid-lubricated cartilage contained a large proportion of cells exhibiting MT depolarization compared to controls (98 ± 2% and 94 ± 4% of cells for 0–50 μm and 50–100 μm for synovial fluid, and 96 ± 3% and 95 ± 14% of cells for 0–50 μm and 50–100 μm for PBS-lubricated cartilage, $p < 0.05$, $n = 4$). Between 100 and 350 μm deep from the articular surface, MT depolarization dropped to 44% and 63% for synovial fluid- and PBS-lubricated cartilage, respectively. These data provide evidence that for sufficiently high friction-induced strains produced by poor lubrication, mitochondrial dysfunction can arise acutely within hours of loading.

Because of the established link between mitochondrial depolarization and apoptosis we determined whether the observed MT depolarization in our tissues is also accompanied by apoptosis (Fig. 2I–L). After sliding, samples were incubated in culture medium for 24 h then assayed for activated caspase 3/7 and counter-imaged using confocal collagen reflectance ($n = 4$ per group). Overall, increased friction promoted chondrocyte apoptosis, as significantly more caspase-positive cells were detected in PBS-lubricated cartilage compared to controls (PBS: 121 ± 88 cells; synovial fluid: 56 ± 30; control 28 ± 18 caspase-positive cells; $p < 0.05$). Similarly to cell death and MT depolarization, apoptosis exhibited significant depth dependence with apoptotic cells found more than 300 μm from the surface in cartilage lubricated by PBS (Fig. 2L). Collectively, these results demonstrate that even in cases where induced strains are sub-necrotic, chondrocytes are still susceptible to adverse responses such as MT depolarization and apoptosis.

3.3. Micro-scale shear strain predicts chondrocyte dysfunction

To quantitatively link the friction induced depth-dependent strains with the cellular responses, we determined whether local strains (Fig. 1) were predictive of cellular dysfunction (Fig. 2). When overlaying shear strain maps on images from our cellular analysis in Fig. 3A, we found a striking visual correlation between the mechanical and biological responses. Further, we binned the frictional shear strain data in the same depth-dependent bins from the cellular analysis to determine correlative relationships. This analysis revealed significant connections between local mechanics and acute cell death. In fact, a weighted sum of shear and normal strain maintained a significant relationship with cell death even with both lubricant groups pooled together ($R^2 = 0.78$, $p < 0.001$, Fig. 3B) establishing a robust connection between friction-induced shear strains and acute cell death. The data further revealed a significant dependence of mitochondrial dysfunction on local mechanics. Plots of the fraction of cells exhibiting mitochondrial depolarization versus local shear strain (Fig. 3C) presented a strong linear correlation between the data sets ($R^2 = 0.95$, $p < 0.00001$) revealing a robust connection between local overload due to strain and mitochondrial function. Similarly, for apoptosis, the correlation between caspase-positive cells and local shear strain provided a strong linear correlation ($R^2 = 0.80$, $p =$

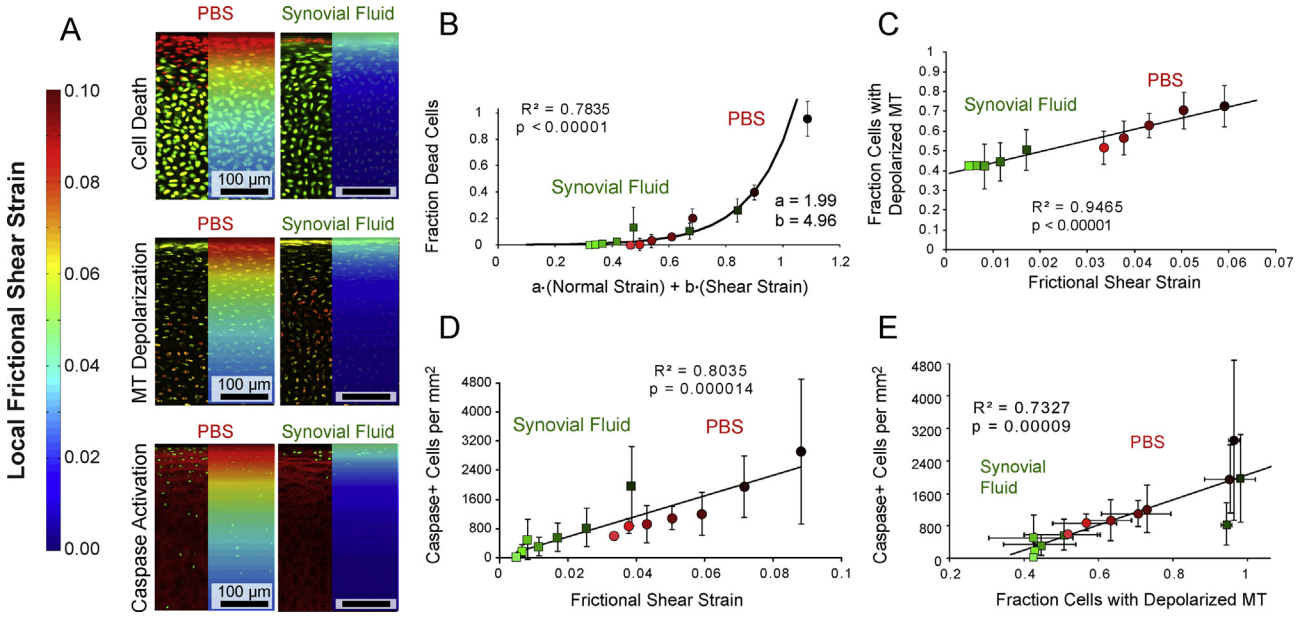

Fig. 3. Microscale characterization of shear strains reveals a strong associated between local mechanics and adverse cellular responses due to friction. (A) Cellular responses are linked to local friction-induced shear strains. (B) Acute cell death correlated highly with a weighted sum of local shear strain and normal strain for both PBS and synovial fluid lubricated cartilage (Exponential curve fit, $R^2 = 0.78$, $p < 0.00001$). (C) MT dysfunction correlated highly with local frictional shear strain ($R^2 = 0.95$, $p < 0.00001$). (D) Number of apoptotic cells correlated highly with local frictional shear strain ($R^2 = 0.80$, $p = 0.000014$). (E) Number of apoptotic cells at 24 h was predicted by MT depolarization at 2 h ($R^2 = 0.73$, $p = 0.00009$).

0.000014, Fig. 3D). Further, the depth-dependent correlation between number of apoptotic cells and MT depolarization was also significant ($R^2 = 0.73$, $p = 0.00009$, Fig. 3E), solidifying the connection between local mechanics, MT depolarization, and apoptosis due to friction induced strain in articular cartilage.

4. Discussion

Collectively, these measurements of cell death, mitochondrial depolarization and apoptosis demonstrate the importance of the friction coefficient in controlling the level of shear strains within cartilage, which in turn influences chondrocyte health. The data revealed distinct mechanisms through which chondrocytes respond to friction in negative ways. In the superficial zone of cartilage where shear strains are amplified, sufficiently large shear strains can result, leaving chondrocytes susceptible to acute death. Additionally, below this surface layer chondrocytes are susceptible to mitochondrial dysfunction and apoptosis in a manner predicted by the local strain (Fig. 3).

The adverse chondrocyte responses described above provide insight into therapeutic interventions for friction-related dysfunction (Fig. 4). One avenue to mitigate the local strains associated with dysfunction is injecting lubricants into the joint space (Balazs and Denlinger, 1993; Flannery et al., 2009; Jay et al., 2010). While lubricant supplementation has been conducted clinically for decades (Balazs and Denlinger, 1993), the present data indicate that altering the lubricating environment can directly alter chondrocyte health. Classically, the effects of elevated friction in arthritis have been considered predominantly mechanical in nature, where elevated friction leads to a wearing away of the cartilage surface in a 'wear and tear' process (Jay et al., 2007; Oungoulian et al., 2015; Radin and Paul, 1971). But, the evidence presented here suggests that acute biological responses to elevated friction also dictate cartilage homeostasis.

While tribosupplementation may reduce friction and consequently the shear strains linked with chondrocyte dysfunction, there are several other therapeutic targets downstream of lowering

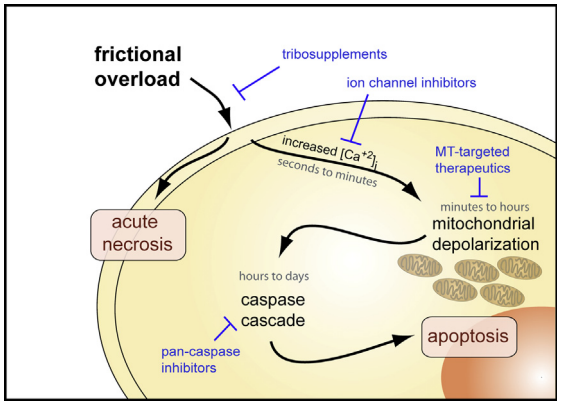

Fig. 4. Chondrocyte responses to frictional overload and targets of therapeutic intervention. In the pathway spanning elevated friction to apoptosis, tribosupplements are an avenue to inhibit frictional overload, ion channel inhibitors can reduce excessive intracellular calcium that promotes mitochondrial depolarization. MT-targeted therapeutics can restore respiratory function and inhibit caspase activation. Finally, pan-caspase inhibitors can inhibit apoptosis, but these therapeutics may not restore respiratory function of chondrocytes.

the friction coefficient. The data from this study implicate mechanotransductive pathways in aberrant responses to friction. While calcium signaling was not explicitly studied here, its role in cartilage mechanotransduction and mitochondrial depolarization is relatively well understood (Huser and Davies, 2007; O'Conor et al., 2014). Indeed, inhibiting calcium signaling in cases of high friction poses a therapeutic target to reduce adverse effects such as MT depolarization and eventual apoptosis, in addition to down regulation of catabolic cytokines (O'Conor et al., 2014). However, it should be noted that as calcium signaling is inhibited, anabolic effects due to mechano-active pathways can also be blocked. Thus, this particular piece of the pathway may be difficult to affect without adverse side effects.

Downstream of calcium signaling, mitochondrial depolarization poses a third therapeutic target to inhibit friction-mediated

chondrocyte dysfunction. While understudied in cartilage, mitochondrial depolarization is implicated in the progression of other diseases including cardiac and neurodegenerative diseases (Levraut et al., 2003; Lin and Beal, 2006). By hindering the function of mitochondria, not only are cellular energetics hindered, but also these dysfunctional cells are typically destined for apoptosis (Wang and Youle, 2009). In line with this train of thought, recent evidence suggests that MT dysfunction is a critical step in the incubation phases of cartilage disease (Delco et al., 2017; Goetz et al., 2016; Waller et al., 2017). In the context of diseases outside of the musculoskeletal umbrella, mitochondrial protection and restabilization has emerged as a tool to halt disease progression or restore organ functionality (Eirin et al., 2014; Szeto, 2008; Szeto and Schiller, 2011). While our group has recently reported on preliminary evidence of mitochondrial protection in cartilage (Delco et al., 2018) the data from the present study indicate that mitochondrial stabilization may pose a robust therapeutic target in cartilage disease or degeneration.

Finally, caspase activation and the apoptotic cascade pose a further downstream therapeutic target as indicated by the present study. As apoptosis has already been implicated in cartilage injury and disease (Hashimoto et al., 1998; Waller et al., 2013), researchers have assessed apoptosis inhibition through pan-caspase inhibitors (D'Lima et al., 2006). While this treatment revealed some degree of damage inhibition, it remained unclear whether the proper function of chondrocytes was maintained in these caspase-blocked cells. Thus, while caspase inhibition may prevent apoptosis, it is possible that a root cause of dysfunction within the mitochondria is not addressed by such treatments, and therefore may not be a robust therapy.

Despite maintaining the well-lubricated surfaces in the vast majority of people, factors such as disease, aging, and injury all adversely affect lubricant levels of articular cartilage. Classically, this increase in friction has been considered a factor leading to 'wear and tear' of the cartilage matrix, but here we have detected clear connections between friction and chondrocyte responses. While frictional overload in this study had the potential to lead to acute necrosis (i.e., shear strain > 0.07), many cells were destined for apoptosis. As such this work establishes additional therapeutic targets aimed at disrupting this cascade. In particular, we are optimistic that emerging therapies aimed at rescuing mitochondrial function could achieve this goal as they have shown promise in treatment of other diseases.

Acknowledgments

This study was supported by the NSF GRFP to EB and LRB, Weill Cornell Medical College Clinical & Translational Science Center Award/National Center for Advancing Translational Sciences (5 UL1 TR000457-09) and The Harry M. Zweig Memorial Fund for Equine Research. IC was supported in part by NSF CMMI 1536463. This research was also supported by NIH 5T32OD011000-20 and NIH 1K08AR068470 to MD, and facilities and instruments used in this study were supported by NIH 1S10RR025502.

Author contributions

EDB, MLD, LAF, IC, and LJB designed the study. EDB and NJ acquired the data. EDB, NJ, and LRB analyzed the data and performed analyses. EDB, IC, and LJB wrote the manuscript. All others were involved in the editing of the manuscript.

Competing financial interests

The authors have no competing financial interests related the work contained within this manuscript.

Appendix A. Supplementary material

Supplementary data associated with this article can be found, in the online version, at https://doi.org/10.1016/j.jbiomech.2018.04.020.

References

Anderson, D.D., Chubinskaya, S., Guilak, F., Martin, J.A., Oegema, T.R., Olson, S.A., Buckwalter, J.A., 2011. Post-traumatic osteoarthritis: improved understanding and opportunities for early intervention. J. Orthop. Res. 29, 802–809. https://doi.org/10.1002/jor.21359.

Ateshian, G.A., 2009. The role of interstitial fluid pressurization in articular cartilage lubrication. J. Biomech. 42, 1163–1176. https://doi.org/10.1016/j.jbiomech.2009.04.040.

Balazs, E.A., Denlinger, J.L., 1993. Viscosupplementation: a new concept in the treatment of osteoarthritis. J. Rheumatol. Suppl. 39, 3–9.

Bartell, L.R., Fortier, L.A., Bonassar, L.J., Cohen, I., 2015. Measuring microscale strain fields in articular cartilage during rapid impact reveals thresholds for chondrocyte death and a protective role for the superficial layer. J. Biomech. 48, 3440–3446. https://doi.org/10.1016/j.jbiomech.2015.05.035.

Bonnevie, E.D., Galesso, D., Secchieri, C., Cohen, I., Bonassar, L.J., 2015. Elastoviscous transitions of articular cartilage reveal a mechanism of synergy between lubricin and hyaluronic acid. PLoS One 10, e0143415. https://doi.org/10.1371/journal.pone.0143415.

Brown, T.D., Johnston, R.C., Saltzman, C.L., Marsh, J.L., Buckwalter, J.A., 2006. Posttraumatic osteoarthritis: a first estimate of incidence, prevalence, and burden of disease. J. Orthop. Trauma 20, 739–744. https://doi.org/10.1097/01.bot.0000246468.80635.ef.

Buckley, M.R., Bergou, A.J., Fouchard, J., Bonassar, L.J., Cohen, I., 2010. High-resolution spatial mapping of shear properties in cartilage. J. Biomech. 43, 796–800. https://doi.org/10.1016/j.jbiomech.2009.10.012.

Buckwalter, J.A., Anderson, D.D., Brown, T.D., Tochigi, Y., Martin, J.A., 2013. The roles of mechanical stresses in the pathogenesis of osteoarthritis: implications for treatment of joint injuries. Cartilage 4, 286–294. https://doi.org/10.1177/1947603513495889.

Carter, T.E., Taylor, K.A., Spritzer, C.E., Utturkar, G.M., Taylor, D.C., Moorman, C.T., Garrett, W.E., Guilak, F., McNulty, A.L., DeFrate, L.E., DeFrate, L.E., 2015. In vivo cartilage strain increases following medial meniscal tear and correlates with synovial fluid matrix metalloproteinase activity. J. Biomech. 48, 1461–1468. https://doi.org/10.1016/j.jbiomech.2015.02.030.

D'Lima, D., Hermida, J., Hashimoto, S., Colwell, C., Lotz, M., 2006. Caspase inhibitors reduce severity of cartilage lesions in experimental osteoarthritis. Arthritis Rheum. 54, 1814–1821. https://doi.org/10.1002/art.21874.

Delco, M.L., Bonnevie, E.D., Bonassar, L.J., Fortier, L.A., 2017. Mitochondrial dysfunction is an acute response of articular chondrocytes to mechanical injury. J. Orthop. Res. https://doi.org/10.1002/jor.23651.

Delco, M.L., Bonnevie, E.D., Szeto, H.S., Bonassar, L.J., Fortier, L.A., 2018. Mitoprotective therapy preserves chondrocyte viability and prevents cartilage degeneration in an ex vivo model of posttraumatic osteoarthritis. J. Orthop. Res. https://doi.org/10.1002/jor.23882.

Eirin, A., Ebrahimi, B., Zhang, X., Zhu, X.-Y., Woollard, J.R., He, Q., Textor, S.C., Lerman, A., Lerman, L.O., 2014. Mitochondrial protection restores renal function in swine atherosclerotic renovascular disease. Cardiovasc. Res. 103, 461–472. https://doi.org/10.1093/cvr/cvu157.

Elsaid, K.A., Fleming, B.C., Oksendahl, H.L., Machan, J.T., Fadale, P.D., Hulstyn, M.J., Shalvoy, R., Jay, G.D., 2008. Decreased lubricin concentrations and markers of joint inflammation in the synovial fluid of patients with anterior cruciate ligament injury. Arthritis Rheum. 58, 1707–1715. https://doi.org/10.1002/art.23495.

Flannery, C.R., Zollner, R., Corcoran, C., Jones, A.R., Root, A., Rivera-Bermúdez, M.A., Blanchet, T., Gleghorn, J.P., Bonassar, L.J., Bendele, A.M., Morris, E.A., Glasson, S.S., 2009. Prevention of cartilage degeneration in a rat model of osteoarthritis by intraarticular treatment with recombinant lubricin. Arthritis Rheum. 60, 840–847. https://doi.org/10.1002/art.24304.

Gleghorn, J.P., Bonassar, L.J., 2008. Lubrication mode analysis of articular cartilage using Stribeck surfaces. J. Biomech. 41, 1910–1918. https://doi.org/10.1016/j.jbiomech.2008.03.043.

Goetz, J.E., Coleman, M.C., Fredericks, D.C., Petersen, E., Martin, J.A., McKinley, T.O., Tochigi, Y., 2016. Time-dependent loss of mitochondrial function precedes progressive histologic cartilage degeneration in a rabbit meniscal destabilization model. J. Orthop. Res. https://doi.org/10.1002/jor.23327.

Griffin, D.J., Vicari, J., Buckley, M.R., Silverberg, J.L., Cohen, I., Bonassar, L.J., 2014. Effects of enzymatic treatments on the depth-dependent viscoelastic shear properties of articular cartilage. J. Orthop. Res. 32, 1652–1657. https://doi.org/10.1002/jor.22713.

Hashimoto, S., Ochs, R.L., Komiya, S., Lotz, M., 1998. Linkage of chondrocyte apoptosis and cartilage degradation in human osteoarthritis. Arthritis Rheum. 41, 1632–1638. https://doi.org/10.1002/1529-0131(199809)41:9<1632::AID-ART14>3.0.CO;2-A.

Huser, C.A.M., Davies, M.E., 2007. Calcium signaling leads to mitochondrial depolarization in impact-induced chondrocyte death in equine articular cartilage explants. Arthritis Rheum. 56, 2322–2334. https://doi.org/10.1002/art.22717.

Jay, G.D., Fleming, B.C., Watkins, B.A., McHugh, K.A., Anderson, S.C., Zhang, L.X., Teeple, E., Waller, K.A., Elsaid, K.A., 2010. Prevention of cartilage degeneration and restoration of chondroprotection by lubricin tribosupplementation in the rat following anterior cruciate ligament transection. Arthritis Rheum. 62, 2382–2391. https://doi.org/10.1002/art.27550.

Jay, G.D., Torres, J.R., Rhee, D.K., Helminen, H.J., Hytinnen, M.M., Cha, C.-J., Elsaid, K., Kim, K.-S., Cui, Y., Warman, M.L., 2007. Association between friction and wear in diarthrodial joints lacking lubricin. Arthritis Rheum. 56, 3662–3669. https://doi.org/10.1002/art.22974.

Kosinska, M.K., Ludwig, T.E., Liebisch, G., Zhang, R., Siebert, H.-C., Wilhelm, J., Kaesser, U., Dettmeyer, R.B., Klein, H., Ishaque, B., Rickert, M., Schmitz, G., Schmidt, T.A., Steinmeyer, J., 2015. Articular joint lubricants during osteoarthritis and rheumatoid arthritis display altered levels and molecular species. PLoS One 10, e0125192. https://doi.org/10.1371/journal.pone.0125192.

Levraut, J., Iwase, H., Shao, Z.-H., Vanden Hoek, T.L., Schumacker, P.T., 2003. Cell death during ischemia: relationship to mitochondrial depolarization and ROS generation. Am. J. Physiol. Heart Circ. Physiol. 284, H549–H558. https://doi.org/10.1152/ajpheart.00708.2002.

Lin, M.T., Beal, M.F., 2006. Mitochondrial dysfunction and oxidative stress in neurodegenerative diseases. Nature 443, 787–795. https://doi.org/10.1038/nature05292.

Murphy, L., Schwartz, T.A., Helmick, C.G., Renner, J.B., Tudor, G., Koch, G., Dragomir, A., Kalsbeek, W.D., Luta, G., Jordan, J.M., 2008. Lifetime risk of symptomatic knee osteoarthritis. Arthritis Rheum. 59, 1207–1213. https://doi.org/10.1002/art.24021.

O'Conor, C.J., Leddy, H.A., Benefield, H.C., Liedtke, W.B., Guilak, F., 2014. TRPV4-mediated mechanotransduction regulates the metabolic response of chondrocytes to dynamic loading. Proc. Natl. Acad. Sci. USA 111, 1316–1321. https://doi.org/10.1073/pnas.1319569111.

Oungoulian, S.R., Durney, K.M., Jones, B.K., Ahmad, C.S., Hung, C.T., Ateshian, G.A., 2015. Wear and damage of articular cartilage with friction against orthopedic implant materials. J. Biomech. 48, 1957–1964. https://doi.org/10.1016/j.jbiomech.2015.04.008.

Radin, E.L., Paul, I.L., 1971. Response of Joints to Impact Loading. I. In Vitro Wear. Arthritis Rheum. 14, 356–362. https://doi.org/10.1002/art.1780140306.

Schmidt, T.A., Gastelum, N.S., Nguyen, Q.T., Schumacher, B.L., Sah, R.L., 2007. Boundary lubrication of articular cartilage: role of synovial fluid constituents. Arthritis Rheum. 56, 882–891. https://doi.org/10.1002/art.22446.

Szeto, H.H., 2008. Mitochondria-targeted cytoprotective peptides for ischemia-reperfusion. Injury. https://doi.org/10.1089/ars.2007.1892.

Szeto, H.H., Schiller, P.W., 2011. Novel therapies targeting inner mitochondrial membrane—from discovery to clinical development. Pharm. Res. 28, 2669–2679. https://doi.org/10.1007/s11095-011-0476-8.

Temple-Wong, M.M., Ren, S., Quach, P., Hansen, B.C., Chen, A.C., Hasegawa, A., D'Lima, D.D., Koziol, J., Masuda, K., Lotz, M.K., Sah, R.L., 2016. Hyaluronan concentration and size distribution in human knee synovial fluid: variations with age and cartilage degeneration. Arthritis Res. Ther. 18, 18. https://doi.org/10.1186/s13075-016-0922-4.

Waller, K.A., Zhang, L.X., Elsaid, K.A., Fleming, B.C., Warman, M.L., Jay, G.D., 2013. Role of lubricin and boundary lubrication in the prevention of chondrocyte apoptosis. Proc. Natl. Acad. Sci. USA 110, 5852–5857. https://doi.org/10.1073/pnas.1219289110.

Waller, K., Zhang, L., Jay, G., 2017. Friction-induced mitochondrial dysregulation contributes to joint deterioration in Prg4 knockout mice. Int. J. Mol. Sci. 18, 1252. https://doi.org/10.3390/ijms18061252.

Wang, C., Youle, R.J., 2009. The role of mitochondria in apoptosis*. Annu. Rev. Genet. 43, 95–118. https://doi.org/10.1146/annurev-genet-102108-134850.

Wong, B.L., Bae, W.C., Chun, J., Gratz, K.R., Lotz, M., Robert, L., Sah, R.L., 2008. Biomechanics of cartilage articulation: Effects of lubrication and degeneration on shear deformation. Arthritis Rheum. 58, 2065–2074. https://doi.org/10.1002/art.23548.